Egyptian Journal of Aquatic Biology & Fisheries
Zoology Department, Faculty of Science,
Ain Shams University, Cairo, Egypt.
ISSN 1110 – 6131
Vol. 29(2): 1493 – 1513 (2025)
www.ejabf.journals.ekb.eg

Implications of Sea Level Change, Tidal Behavior, and Storm Surges at Port Said Harbor, Egypt

Mohamed A. Abdul-Qader[1], Ahmed M. Khedr[1], Tarek M. El-Geziry[2]*

[1]Arab Academy for Science, Technology and Maritime Transport, AASTMT, Alexandria, Egypt
[2]National Institute of Oceanography and Fisheries, NIOF, Cairo, Egypt

***Corresponding Author:** tarekelgeziry@yahoo.com

ARTICLE INFO

Article History:
Received: Feb. 2, 2025
Accepted: March 25, 2025
Online: April 2, 2025

Keywords:
Port-Said Harbor,
Egypt,
Sea level,
Meteorological conditions,
Tidal analysis,
Surge dynamics

ABSTRACT

A detailed analysis of sea level variations at Port Said Harbor, Egypt, was conducted using hourly data from a radar water level sensor collected between May 2018 and February 2023. Surge elevations were calculated by subtracting the astronomical height from the observed sea level using the T_TIDE package, which was also applied to perform harmonic analysis and to calculate tidal datums, revealing a semidiurnal tidal regime with an F-factor of 0.215. Tidal influences accounted for only 1.34% of the observed sea level variations, while surge dynamics, primarily driven by atmospheric pressure and wind components, accounted for the remaining 98.66%. The mean sea level (MSL) was 70.36cm, while the mean tide level (MTL) was 70.33cm, 3cm lower than MSL. The spring-to-neap ratio was approximately 4.06, with M_2, S_2, and Sa having the largest amplitudes among the resulting 68 tidal constituents. Higher atmospheric pressure was linked to slightly lower surge heights, and wind speed components showed weak negative correlations, with horizontal wind speed (Wx) at -0.14 and vertical wind speed (Wy) at -0.12, indicating a mild association between higher wind speeds and lower surge levels. The study provides the empirical equation relating surge height to varying atmospheric pressure and wind speed.

INTRODUCTION

Almost half the world's population lives within 100km of the sea, with approximately 90% of global trade conducted through maritime routes **(Pugh & Woodworth, 2014)**. Sea level dynamics range from short-term tidal cycles to long-term changes driven by geology and climate **(Manual on Sea-Level Measurements and Interpretation, 2006)**. Over the past century, global mean sea level (MSL) has risen at an accelerating rate, from 1.4mm/ year during the 20th century to 3.3mm/ year between 1993 and 2020, and 4.4mm/ year from 2013 to 2021, primarily due to ice sheet melting and thermal expansion **(Watson *et al*., 2021; UNEP, 2021)**. This rise increases risks such as flooding, erosion, and saltwater intrusion, affecting coastal areas worldwide **(Church *et al*., 2013)**. The Mediterranean Sea, a semi-enclosed basin, exhibits unique sea level characteristics influenced by global and regional factors. Studies have revealed a positive sea level rise (SLR) trend attributed to thermal expansion and climate variability. **Cazenave *et al*. (2001)** reported a rise in the Mediterranean's sea level, primarily driven by thermal expansion during the late 20th century. Long-term sea level fluctuations in the Eastern Mediterranean (1923–2019) were analyzed using Permeant Service for Mean Sea Level (PSMSL) data **(Ibrahim & El-Gindy, 2022)**. Their results revealed a higher rise in non-linear projections than linear ones, with dominant 12-month seasonal (40.24–83.33 mm) and 11-year solar (6.74–35.6mm) cycles. Phase delays reached 2.35 months east-west and 0.61 months north-south in the Levantine Sea. Future sea level rise estimates support risk assessment and adaptation planning. The sea level variation along the Egyptian Mediterranean coast results from the combined effects of astronomical tides and surge elevations. Tides are mainly semidiurnal, with a dominant tidal range in the order of a few centimetres **(Hussein *et al*., 2010; Saad *et al.*, 2011; El-Gezirу & Radwan, 2012)**. Surges affected by meteorological conditions may reach a height of 1.0m **(El-Gezirу & Radwan, 2012)**, and therefore, have more impact on the coast. Recently, **Alam El-Din *et al*. (2019)** analyzed data spanning 1993 to 2015, showing an absolute SLR rate of 0.5 to 5.5mm/ year in the Southern Levantine region of the Mediterranean. **Shalaby (2000)** studied surge phenomena along the Egyptian Mediterranean coast, highlighting seasonal variations in surge magnitudes. Positive surges, with sea levels rising over 25cm, were observed in winter, while negative surges, with sea levels dropping as low as -29cm, occurred in spring. **El-Gezirу (2020)** noted a declining sea-level gradient along the Egyptian Mediterranean coast from east to west, with MSL ranging between 32 and 67cm.

Port Said Harbor is located at the northern entrance of the Suez Canal on the Mediterranean coast of Egypt, (Fig. 1). Geographically, it lies between latitudes 31° 15' N and 31° 17' N and longitudes 32° 15' E and 32° 20' E. It covers 25km² with an 8km coastline, with depths ranging from 10m in inner areas to 18m at the main entrance channel, accommodating large vessels **(Egyptian General Authority for Shore Protection, 2015)**. This strategic position allows Port Said to act as a crucial maritime hub, linking the Mediterranean Sea with the Red Sea via the Suez Canal. Established in 1859 during the canal's construction, Port Said City has grown significantly, with a population of approximately 797,000 people as of recent estimates **(UNCTAD, 2021)**. The variations in sea level at Port Said were intensively examined. **Mobarek and Anis (1974)** reported water levels ranging from 60cm highest high-water level (HHWL) to -20cm lowest low-water level (LLWL) relative to the datum (1926–1973). **Sharaf El Din *et al*. (1989)** found an average level of 49.6cm above the same datum, with seasonal highs in summer and lows in winter. **El Fishawi (1993)** observed a 1.3mm/ year SLR trend (1926–1987), aligning with **Shaker *et al*. (2009)**. **Eid *et al.* (1997)** noted July–November seasonal peaks and an average level of 61cm. **Moursy (1998)** and **Radwan *et al*. (2021)** confirmed the semi-diurnal tide pattern, with M_2, S_2, amplitudes of 7.4 and 4.4cm. **Frihy *et al.* (2010)** recorded a 2.87mm/ year SLR rate, influenced by global climate and local subsidence. Vulnerability studies, including **El-Raey *et al.* (1999)**, warn of economic losses and displacement with SLR scenarios of 0.5–1.25m. **El-Geziry and El-Wakeel (2023)** initiated a comprehensive study utilizing sea-level recording devices and a dataset covering a decade (2002–2011) of hourly sea-level records at Port Said Harbor. Their research investigated sea-level variability, MSL, and annual rate trends. The hourly measurements observed for Port Said Harbor exhibited fluctuations ranging from 4.3 to 116.3cm, with an MSL recorded at 69.1cm, which is slightly higher than **Moursy's (1998)** calculation, reflecting the annual increase. These findings are also consistent with **El-Geziry and Said (2020)**, who concluded the MSL was 67cm. The lowest levels occurred in the spring months (March-May), while the highest levels were observed in summer (July and August), aligning with findings by **Eid *et al.* (1997)** and **Moursy (1998)**. According to **WMO (2024)**, the climate in Port Said exhibits typical Mediterranean characteristics, with hot summers (36-38°C) and mild winters (23-26°C), while occasional extreme weather events may occur. **Khedr and Helmy (2024)** utilized hourly sea-level data at Port Said Harbor, analyzing five years of data (June 2010 to June 2015). They revealed that semi-diurnal constituents (M_2, S_2) and the seasonal constituent solar annual (Sa) dominate tidal behavior, with tidal asymmetry indicating a short flood tide. The study also found a small positive 2 mm/year trend in sea-level rise from 2011 to 2015.

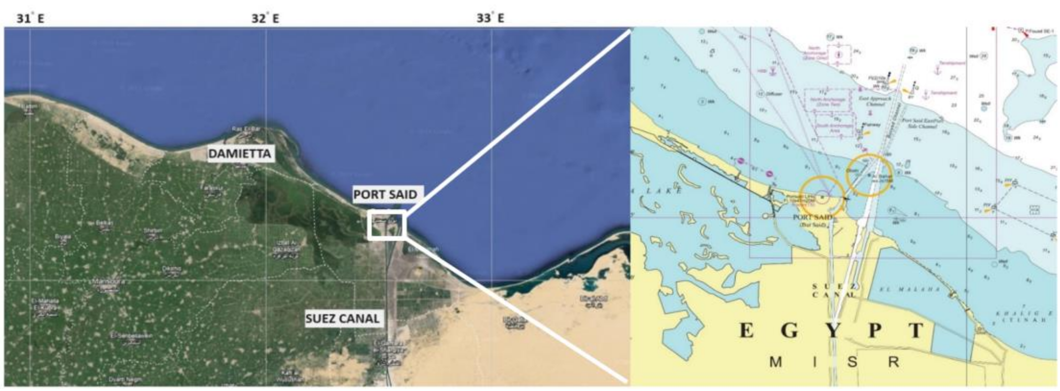

Fig. 1. Location map for Port Said harbor located on the Mediterranean coast **(Google Earth, 2024)**, illustrated on M23 Nautical chart of Port Said **(ENHD, 2024)**

While previous studies have examined sea level variations along the Egyptian Mediterranean coast, they were often constrained by limited temporal coverage, reliance on older tide gauge equipment, and a lack of comprehensive integration with meteorological influences. Furthermore, earlier research centered mostly on defining tidal patterns and astronomical constituents, with little emphasis on estimating the extent of surge contributions. For instance, studies such as **El-Geziry and Said (2020)** and **Radwan *et al.* (2021)** identified long-term trends but lacked comprehensive empirical modeling of surge influences. This study fills these gaps by examining a new, high-resolution dataset (2018-2023), applying sophisticated harmonic analysis techniques, and adding meteorological correlations to improve forecasts of sea level variability and surge behavior. By refining tidal datum calculations and developing an empirical equation to predict surge heights, this research enhances the understanding of sea level fluctuations, offering critical insights for navigation safety, flood risk management, and coastal infrastructure resilience at Port Said Harbor. These enhancements provide more precise insights into coastal infrastructure development, navigation safety, and flood risk management in the region.

The present work aimed to update the general behavior of sea-level variations in Port Said Harbor by analyzing hourly sea-level data collected from the newly installed radar system, spanning the period between 2018 and 2023. This study developed a robust understanding of these variations by examining tidal and surge characteristics and correlating them with meteorological conditions. Moreover, it provided the empirical equation relating variations in surge elevations to atmospheric pressure and wind speed. The obtained results will provide accurate insights to support multiple applications, including hydrographic surveys, navigation through shallow channels, flood warning systems, and the design and operation of coastal and offshore structures. These findings will improve the Suez Canal entrance and its waiting area’s operations and will ensure safe and efficient maritime activities.

MATERIALS AND METHODS

Sea level data

Sea level data were collected using a CS475A radar water level sensor at coordinates (31°15′16.74″N, 032°18′10.48″E), (Fig. 2), in Port Said Harbor, referenced to the Egyptian Survey Authority (ESA) zero datum, where the ellipsoidal height of the zero datum is 16.22 meters. Over 4 years and 8 months (May 2018–February 2023), 41413 hourly observations were recorded, with 37699 hours (91%) usable after addressing technical issues. This dataset supports analyzing tidal influences, and surge events with their meteorological causes.

Metrological data

The predictable pattern of tides is often disrupted by atmospheric pressure and winds, resulting in surges that can cause significant sea level variations and, historically, coastal flooding during high tides **(Pugh, 1987)**. Meteorological data, including air temperature (T2m), wind speed, and direction (U10, V10), were collected from the Automated Weather Observing System (AWOS) at Port Said International Meteorological Station, (Fig. 2), over nearly five years (May 21, 2018–February 9, 2023), coinciding with the sea level data period. With 41,413 recorded hours and 99.7% data availability.

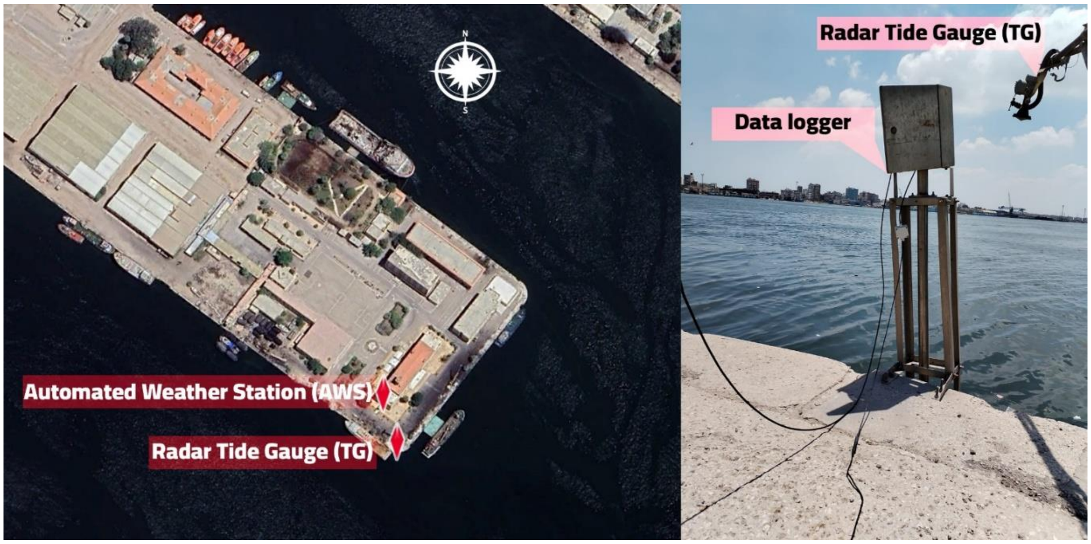

Fig. 2. Map of the geographic position of the water level sensor and the automated weather station at Port Said Harbor **(Google Earth, 2024)**

Methods of analysis

Sea level data were organized and smoothed using Microsoft Excel® 2019 to facilitate statistical analyses. Descriptive statistics, including minimum, maximum, range, mean, and standard deviation, were calculated annually. The MSL, derived from hourly records, was further analyzed for annual trends and monthly variations. Tidal elevations, along with astronomical amplitudes and phases, were obtained through harmonic analysis using the T-TIDE package in MATLAB® R2021a. This package uses typical harmonic analysis to produce astronomical constituents, depending on the given data quality, data period, and geographical location **(Pawlowicz *et al*., 2002)**. It was also used to separate tidal elevations and residuals (surge) from the original sea level data. This approach was previously applied by **Svensson and Jones (2004)**, **El-Geziry and Radwan (2012)** and **El-Geziry and El-Wakeel (2023)**. The elevation at any time (t) was calculated using the equation:

$$x(t) = b_0 + b_1 t + \sum_{k=1,\dots,N} a_k e^{i\sigma_k t} + a_{-k} e^{-i\sigma_k t} \qquad (1)$$

Where, b_0 is a constant offset; b_{1t} accounts for a possible linear trend; N is the number of tidal constituents; a_k and a_{-k} are the complex amplitudes of each tidal constituent; σ_k is the known frequency of each constituent (based on astronomical considerations). The primary tidal constituents (O_1, K_1, M_2, S_2) were calculated through the harmonic tidal analysis. The Signal to Noise Ratio (SNR), calculated as the squared ratio of amplitude to amplitude error, was a key output. Simulations in t_synth (detailed in t_errors) showed that SNR variability aligned with confidence intervals. The linear SNR method is accurate for real-time series (e.g., tidal height) when SNR > 10, and remains reliable down to 2 or 3. The non-linear method provides better accuracy at lower SNR. Constituents with an SNR > 1 are considered significant, indicating meaningful tidal components **(Pawlowicz *et al*., 2002)**. The results were then utilized to classify the tidal cycle using **Pugh (2004)** constituent factor determined by the following equation:

$$FF= (H_{O1}+H_{K1})/(H_{M2}+H_{S2}) \qquad (2)$$

Where, FF is the f-factor ratio of diurnal to semidiurnal tidal constituents; H_{O1} is the tidal height of the principal lunar diurnal constituent; H_{K1} is the tidal height of the luni-solar diurnal constituent; H_{M2} is the tidal height of principal lunar semi-diurnal constituent; H_{S2} is the tidal height of principal Solar semi-diurnal constituent. A tidal cycle is defined as semidiurnal if the FF ratio falls between 0 and 0.25, mixed mainly semidiurnal if the FF ranges from 0.25 to 1.25, mixed mainly diurnal if the ratio is between 1.25 and 3, and diurnal if it exceeds 3 **(Pugh & Woodworth, 2014)**. Furthermore, the astronomical results were used to calculate various theoretical principal terms associated with the tidal phenomenon at the harbor, such as the HHWL, the LLWL, and the maximum tidal range, following the methodology of **Doodson (1957)**.

The correlation between meteorological parameters (air temperature, atmospheric pressure, and wind speed components) and sea level was analyzed using Microsoft Excel® 2019 and WRPLOT View (version 8.0.2), which helped assess the influence of wind regimes and pressure on sea-level variations. The impact of wind speed components and sea-level pressure (SLP) on surge behavior was examined by establishing correlations between these three meteorological elements and the heights of total, positive, and negative surges. The wind data were also analyzed, with respect to the true north, by decomposing it into two components: Wx, the wind blowing along the coastline, and Wy, which is the wind blowing directly toward or away from the coast, using the same approach that has been previously employed by **El-Geziry and Dabbous (2021)**, by using the following equations:

$$W_x = W \sin [(\phi +180) \times 3.14/180] \qquad (3)$$

$$W_y = W \cos [(\phi +180) \times 3.14/180] \qquad (4)$$

Where, W_x and W_y are the parallel and perpendicular wind components, respectively (m/s); W is the total wind speed recorded at the meteorological station (m/s); $\emptyset$ is the wind direction measured from the True North (°).

RESULTS AND DISCUSSION

1. Sea level characteristics in Port Said Harbor

The analysis of sea level data showed an MSL of 70.36cm (Fig. 3). **Eid *et al.* (1997)** reported an MSL of 61cm, while **El-Geziry (2020)** recorded 67cm, closely aligning with these findings. Similarly, **El-Geziry and El-Wakeel (2023)** observed a slightly higher MSL of 69.1cm during 2002–2011. Monthly variations (Fig. 4) indicated higher sea levels in summer (e.g., July and August) and lower levels in winter (e.g., February and March). This seasonal pattern was consistent with findings by **Sharaf El Din *et al.* (1989)** and **Eid *et al.* (1997)**, who also noted higher summer levels and lower winter levels. **El-Geziry and El-Wakeel (2023)** reported similar seasonal trends, supporting this study's results. **Alam El-Din *et al.* (2007)** observed identical seasonal oscillations, with high summer and low winter levels and a positive sea level trend of 2.87mm/ year. This seasonal behavior is in accordance with the atmospheric pressure scheme affecting the eastern Mediterranean basin, described by **Tsimplis *et al.* (2005)**, **Gomis *et al.* (2008)** and **Oddo *et al.* (2014)**.

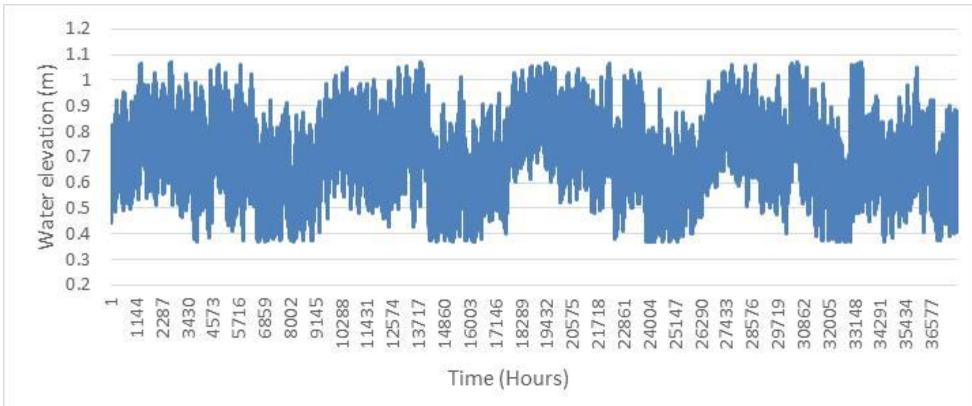

Fig. 3. Observed sea level data set during the study period measured by radar water-level sensor at Port Said Harbor

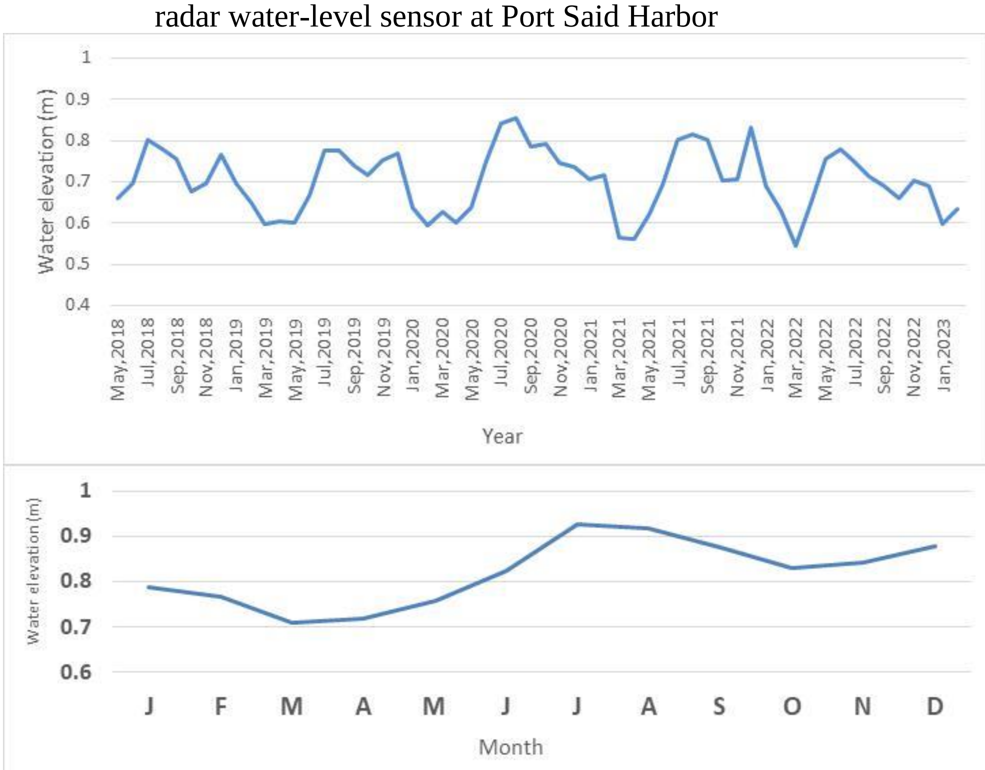

Fig. 4. Monthly mean sea level (MMSL) and seasonal variability during the study period

2. Principal characteristics of tides in Port Said Harbor

A harmonic analysis resulted in 68 tidal constituents. Of these, 23 were found significant at the 95% confidence level as marked with an asterisk (Table 1). The tidal signal obtained from harmonic analysis and residual signal are depicted in Fig. (5). To identify the dominant tide type in the study area, the F-factor was calculated to be 0.215. This F-factor value indicated that the tidal regime in the study area is primarily semidiurnal, with semidiurnal components (M_2, S_2) being more dominant than diurnal components. This result closely aligns with previous findings: **Moursy (1998)** identified a semidiurnal tide dominated by (M_2, S_2), while **Tonbol and Shaltout (2013)** calculated an F-factor of 0.23 also indicating a semidiurnal cycle. **Khedr *et al.* (2022)** reported an F-factor of 0.21, confirming a semidiurnal regime. **Helmy and Khedr (2024)** similarly calculated an F-factor of 0.21, supporting the dominance of semidiurnal tides. **El-Geziry and El-Wakeel (2023)** described the tidal cycle at Port Said as mixed but mainly semidiurnal. The current study's F-factor of 0.215 aligns well with these consistent findings. Fig. (6) provides a visual representation of the amplitudes of the astronomical tidal constituents, illustrating that M_2, Sa, and S_2 have the highest amplitudes among them. This graph complements (Table 1) by clearly highlighting the relative strength of each constituent in a visual format. In Table 2, a comparison of the primary tidal constituents (M_2, S_2, K_1, and O_1) for Port Said Harbour is presented, drawing on data from multiple studies.

Table 1. Significant tidal constituents constructed by the T_TIDE package at Port Said

Constituents	Frequency (Cycle/hr)	Amplitude (cm)	Phase (deg)	Constituents	Frequency (Cycle/hr)	Amplitude (cm)	Phase (deg)
***SA**	0.0001141	**9.09**	250.71	***M2**	0.0805114	**10.11**	306.89
***SSA**	0.0002282	5.21	220.29	***H2**	0.0806255	0.29	169.42
***MSM**	0.0013098	1.18	334.44	***MKS2**	0.0807396	0.15	92.14
MM	0.0015122	0.58	71.24	***LDA2**	0.0818212	0.13	267.82
MSF	0.0028219	0.58	319.51	***L2**	0.0820236	0.55	324.89
MF	0.0030501	0.15	122.65	***T2**	0.0832193	0.48	19.57
ALP1	0.0343966	0.06	127.15	***S2**	0.0833333	**6.11**	321.25
2Q1	0.0357064	0.05	310.93	***R2**	0.0834474	0.32	12.39
SIG1	0.0359087	0.01	156.69	***K2**	0.0835615	1.79	315.26
***Q1**	0.0372185	0.19	253.06	***K2**	0.0835615	1.66	343.65
***RHO1**	0.0374209	0.07	302.03	**MSN2**	0.0848455	0.08	225.76
***O1**	0.0387307	1.49	276.51	***ETA2**	0.0850736	0.09	13.83
***TAU1**	0.0389588	0.07	140.38	***MO3**	0.1192421	0.10	83.48
BET1	0.0400404	0.06	284.46	***M3**	0.1207671	0.27	107.75
***NO1**	0.0402686	0.12	303.08	***SO3**	0.1220640	0.08	190.08
***CHI1**	0.0404710	0.08	194.66	***MK3**	0.1222921	0.04	125.89
***PI1**	0.0414385	0.14	278.87	***SK3**	0.1251141	0.15	20.04
***P1**	0.0415526	0.63	313.80	***MN4**	0.1595106	0.10	74.90
***P1**	0.0415526	0.68	311.66	***M4**	0.1610228	0.11	136.65
***S1**	0.0416667	0.99	317.63	**SN4**	0.1623326	0.01	34.06
***K1**	0.0417807	2.05	304.59	***MS4**	0.1638447	0.05	133.02

***PSI1**	0.0418948	0.13	105.10	***MK4**	0.1640729	0.14	203.82
***PHI1**	0.0420089	0.11	21.88	***S4**	0.1666667	0.07	10.56
THE1	0.0430905	0.05	49.57	***SK4**	0.1668948	0.05	234.50
***J1**	0.0432929	0.13	303.00	***2MK5**	0.2028035	0.06	30.55
SO1	0.0446027	0.05	82.69	***2SK5**	0.2084474	0.05	91.12
***OO1**	0.0448308	0.10	283.52	***2MN6**	0.2400221	0.09	92.65
UPS1	0.0463430	0.04	315.06	***M6**	0.2415342	0.16	128.77
OQ2	0.0759749	0.08	357.37	***2MS6**	0.2443561	0.19	170.53
***EPS2**	0.0761773	0.15	310.50	**2MK6**	0.2445843	0.05	160.68
***2N2**	0.0774871	0.35	320.00	***2SM6**	0.2471781	0.05	238.53
+	0.0776895	0.24	335.08	***MSK6**	0.2474062	0.06	255.21
***N2**	0.0789992	1.68	317.82	***3MK7**	0.2833149	0.05	97.93
***NU2**	0.0792016	0.42	302.00	***M8**	0.3220456	0.04	96.27
***GAM2**	0.0803090	0.18	85.98	**M10**	0.4025570	0.01	61.87
***H1**	0.0803973	0.44	229.52				

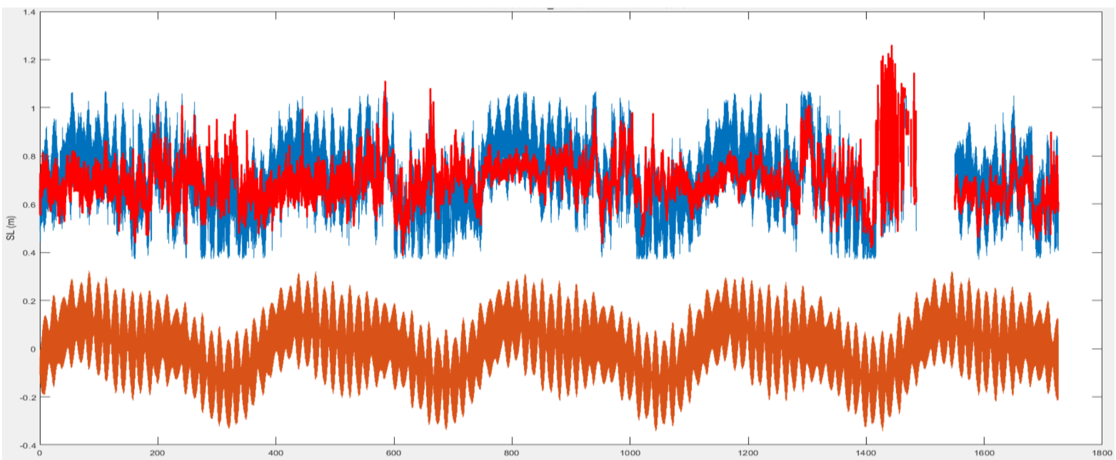

Fig. 5. Observed – harmonic - residual from harmonic analysis from May 2018 to Feb 2023

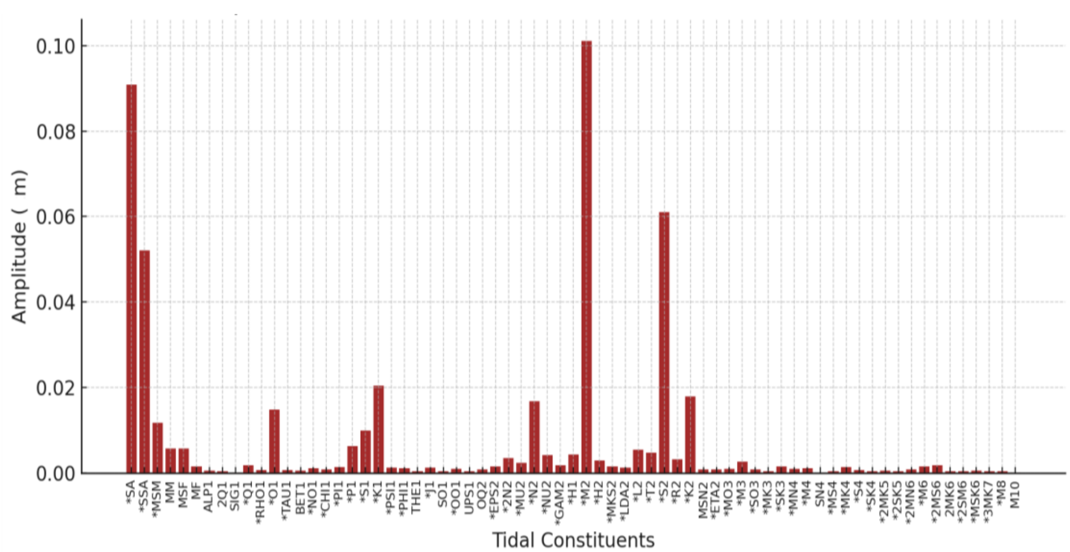

Fig. 6. Amplitudes of the constructed astronomical tidal constituents

Table 2. Comparative summary of tidal constituents' amplitudes and phases at Port Said

Study	Constituent	Amplitude (cm)	Phase (degrees)	Year/Period
Defant (1961)	M2	11.7	304	1961
	S2	6.9	319	1961
	K1	2.1	305	1961
	O1	1.7	275	1961
Moursy (1998)	M2	11.1	305	1986
	S2	7	315	1986
	K1	2	307	1986
	O1	1.5	280	1986
Tonbol & Shaltoot (2013)	M2	10.4	169.77	1999-2000
	S2	6.2	237.2	1999-2000
	K1	2.2	255.89	1999-2000
	O1	1.6	192.28	1999-2000
El-Geziry & El-Wakeel (2023)	M2	13.4	322.76	2002-2011
	S2	2.2	250	2002-2011
	K1	3.1	8.16	2002-2011
	O1	1.15	258.83	2002-2011
Radwan *et al.* (2021)	M2	11.32	336.48	2015
	S2	6.694	308.189	2015
	K1	1.751	295.205	2015
	O1	1.453	309.215	2015
Khedr *et al.* (2022)	M2	11.24	296	2015
	S2	6	309	2015
	K1	2.15	299	2015
	O1	1.66	271	2015
Helmy and Khedr (2024)	M2	11.23	234.86	2010-2015
	S2	6.85	308.64	2010-2015
	K1	2.17	121.42	2010-2015
	O1	1.65	26.8	2010-2015
Current Study	M2	10.11	306.89	2018-2023
	S2	6.11	321.25	2018-2023
	K1	2.05	304.59	2018-2023
	O1	1.49	276.51	2018-2023

Descriptive statistics of tides showed a mean tidal elevation of 0.6cm, with a maximum of 32.3cm and a minimum of -34.3cm, resulting in a tidal range of 67cm. MSL is defined as the average of hourly sea level measurements over an extended period, ideally at least one year, to account for long-term cycles, while the Mean Tidal level (MTL) represents the midpoint between the Highest High Water Level (HHWL) and Lowest Low Water Level (LLWL), considering shallow water effects **(Pugh & Woodworth, 2014)**. In this study, MSL was calculated as 70.36cm, while MTL was 70.33cm, 3cm lower than MSL. These values were determined using Equation 5 from **Moursy (1998)**, **El-Geziry *et al.* (2021)** and data from Table (1).

$$\text{MTL}= \text{MSL} + M_4 \cos(2M_2° - M_4°) - \left[\frac{0.04(K_1+O_1)^2}{M_2}\right]\cos\,(M_2° - K_1° - O_1°) \quad (5)$$

Where, MTL is the Mean Tide Level, representing the adjusted average sea level considering tidal influences; MSL is the Mean Sea Level, the baseline average sea level; M_4 is the amplitude of the M_4 tidal constituent, corresponding to the quarter-diurnal tidal component; $M_2°$ is the phase angle of the M_2 constituent, indicating the phase position in the tidal cycle for the principal lunar semidiurnal tide; $M_4°$ is the phase angle of the M_4 constituent, showing the phase position for the quarter-diurnal tide; K_1 is the amplitude of the K_1 tidal constituent, representing a diurnal tide mainly influenced by both the moon and the sun; O_1 is the amplitude of the O_1 tidal constituent, representing another diurnal component due primarily to lunar gravitational forces; $K_1°$ is the phase angle of the K_1 constituent, indicating its phase position in the tidal cycle; $O_1°$ is the phase angle of the O_1 constituent, indicating its position within the cycle.

The fact that the MTL is lower than the MSL aligns with the conclusions of this research, which attributes this difference primarily to the dominance of meteorological effects over astronomical influences. Specifically, the presence of positive surges without any recorded negative surges contributes significantly to the 3cm difference. Additionally, the asymmetry in the tidal cycle, driven by the dominance of the semi-diurnal constituents (M_2 and S_2) and their phase interactions, results in more pronounced low tides compared to high tides, ultimately lowering MTL relative to the MSL.

3. Tidal datum realization

The tidal datum levels were determined through harmonic analysis of observed sea level data, using the amplitudes of the four primary tidal constituents (M_2, S_2, K_1, O_1) based on theoretical formulas derived from harmonic principles **(Doodson, 1957)**. The equations applied in these calculations, along with the resulting values for each tidal datum and a comparison between the results of the current study and those of **El-Geziry and El-Wakeel (2023)**, are presented in Table (3). The calculated spring-to-neap ratio was approximately 4.06.

Table 3. Theoretical characteristics of tides at Port Said

Tidal datum	Equation	Current study's result (cm)	El-Geziry and El-Wakeel (2023)
Year/Period	-	2018-2023	2002-2011
Mean Sea Level (MSL)	-	70.36	69.1
Mean High Water Spring (MHWS)	MSL + (M_2+ S_2)	86.58	84.8
Mean Low Water Spring (MLWS)	MSL - (M_2 + S_2)	54.14	53.4
Mean Spring Range (MSR)	2 * (M_2 + S_2)	32.44	31.4
Mean High Water Neap (MHWN)	MSL + (M_2 - S_2)	74.36	80.4
Mean Low Water Neap (MLWN)	MSL - (M_2 - S_2)	66.36	57.8
Mean Neap Range (MNR)	2 * (M_2 - S_2)	08.00	22.6
Highest High Water Level (HHWL)	MSL + (M_2 + S_2 + O1 + K1)	90.12	89.1
Lowest Low Water Level (LLWL)	MSL - (M_2 + S_2 + O1 + K1)	50.60	49.1
Highest Range of Tides (HRT)	2 * (M_2 + S_2 + O1 + K1)	39.52	40.0

4. Surges and metrological conditions

4.1. Metrological conditions

The air temperature analysis recorded a daily minimum of 6.4°C, and a maximum of 37.2°C, with a mean daily temperature of 22.32°C. Lower temperatures occurred more frequently than extreme highs. These findings align with **WMO (2024)**, which reported typical summer highs of 36-38°C, consistent with this study's 37.2°C, particularly in July and August. However, winter temperatures in this study (13-17°C) were lower than WMO's range of 23-26°C. Temperatures peaked during summer (June-August) at 28-29°C, especially in July and August, and dropped to 13-17°C in winter (December-February), consistent with **El-Ashmawy *et al*. (2017)**. Despite minor variations, seasonal patterns of warmer summers and cooler winters were observed, as shown in Fig. (7), indicating a cyclical trend. At the same time, the overall mean atmospheric pressure was 1014.97 hPa. Monthly averages showed a clear seasonal pattern, with higher pressure in cooler months and lower pressure in warmer months (Fig. 8). Similar to **Alam El-Din *et al.* (2007)**, pressure dipped to around 1012.6 hPa in summer (e.g., July and August) and peaked at 1016-1017 hPa in winter (e.g., December and January). A comparison of air temperature and atmospheric pressure (Fig. 9) revealed an inverse relationship: higher temperatures in warmer months corresponded to lower pressures, while colder months showed higher pressures. This pattern aligned with **Alam El-Din *et al.* (2007)**, who observed seasonal temperature oscillations inversely related to atmospheric pressure. Similar seasonal fluctuations in both parameters were evident in this study, with pressure dropping during warmer months and rising during cooler months.

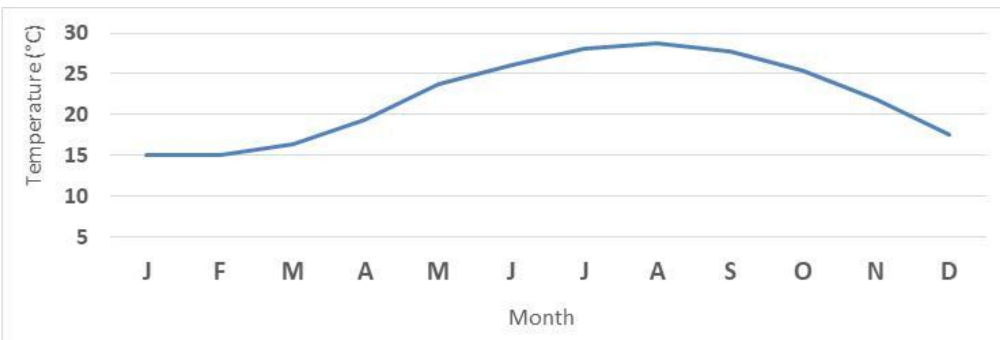

Fig. 7. Seasonal variability of temperature along Port Said

Fig. 8. Seasonal variability of atmospheric pressure along Port Said

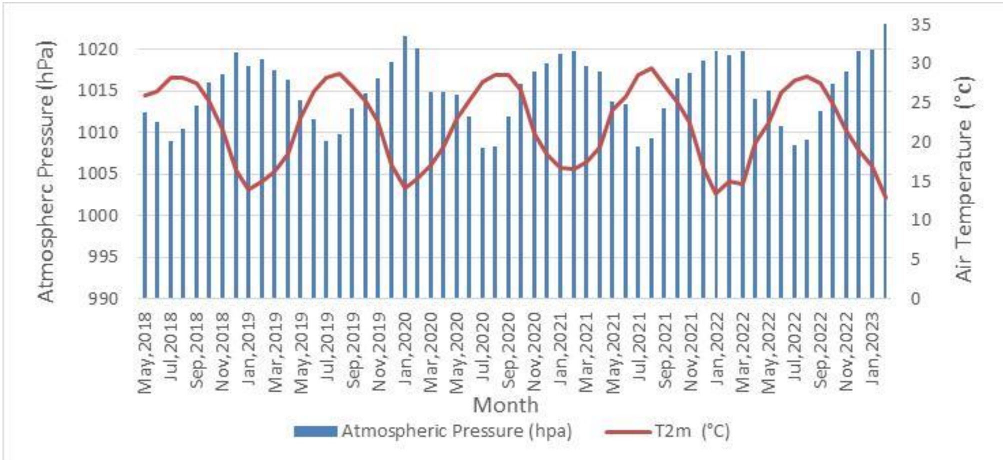

Fig. 9. Monthly means of air temperature (C) and atmospheric pressure (hPa) indicated the inverse relationship at Port Said during the study period

The wind speed data showed a maximum of 33m/ s, a minimum of 0m/ s, and an average of 8.8m/ s. Calm conditions (wind speeds below 0.49 m/s) occurred 4.03% of recorded hours. The parallel-to-coast wind speed ($W_{x)}$ values ranged from -4.94 to 3.86m/ s, and the vertical-to-coast wind speed (Wy) from -16.26 to 13.59m/ s. W_y had a stronger coastal impact, pushing water toward the shore and increasing the risk of flooding and erosion, especially during strong onshore winds. Managing perpendicular winds was crucial for protecting the coastline and harbor. The wind rose analysis (Fig. 10) showed that the prevailing wind direction at Port Said was primarily from the north, with strong winds (above 11.1m/ s) originating from the north and northwest. This pattern aligned with typical Mediterranean wind trends. Similarly, **Alam El-Din *et al.* (2007)** identified dominant northern winds with occasional northwest winds, consistent with these findings. **El-Ashmawy *et al.* (2017)** also reported prevailing northwesterly winds, the "Mediterranean Sea Breeze," which accounted for 13.6% of this study's recorded winds.

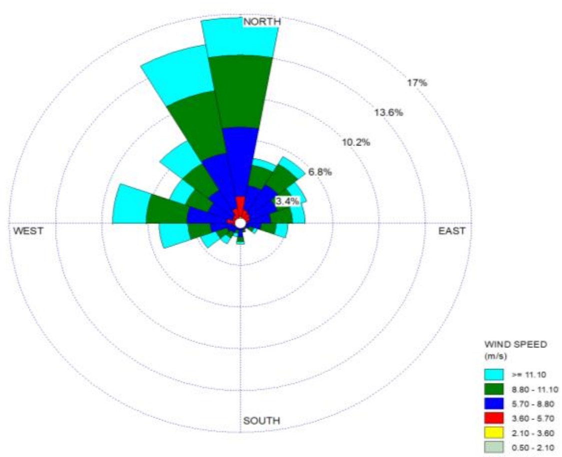

Fig. 10. Wind rose for the prevailing wind regime over the study period at Port Said

4.2. Surge heights

The analysis of surge heights revealed that surge dynamics significantly influenced sea level variations. Surge levels ranged from a high of 126cm to a low of 38.5cm, with a mean of approximately 69.6cm. Fig. (11) illustrates the surge height distribution, showing a dominance of positive surge levels and no negative surges recorded during the study period. Monthly surge statistics capture seasonal trends, with relatively stable surge levels across the months (Fig. 12).

Surge effects contributed 98.66% to the observed sea level variations, while tidal influences accounted for only 1.34%, highlighting the dominance of surge dynamics at Port Said. With minimal tidal influence, this surge-driven pattern aligns with **El-Geziry and El-Wakeel (2023)**, who found the astronomical tide contributed 2.3% and the surge 97.7%, further emphasizing the prominence of surge effects in the region.

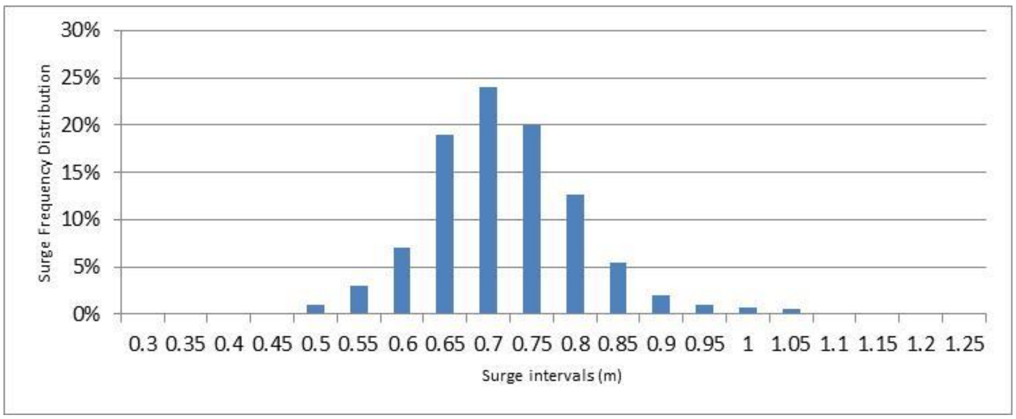

Fig. 11. Surge frequency distribution (%) over the study period at Port Said

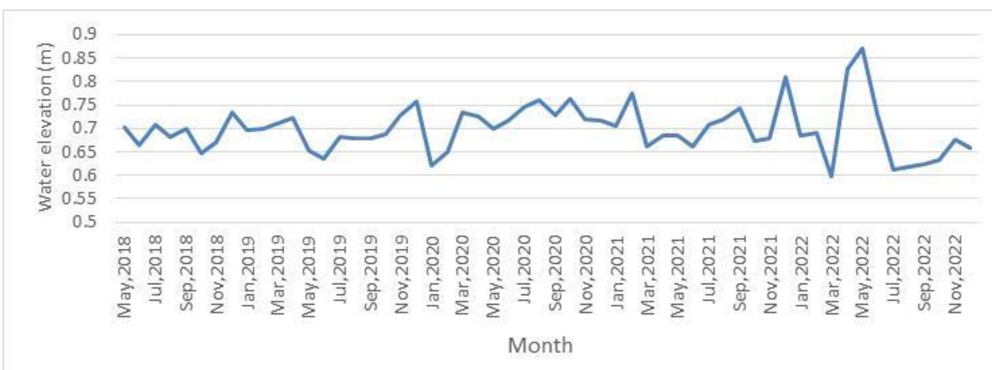

Fig. 12. Monthly average surge heights over the study period at Port Said

4.3. Correlation to metrological conditions

The correlation analysis of surge heights with meteorological parameters (Table 4) revealed that atmospheric pressure had the strongest influence, with a negative correlation of -0.18, indicating that higher atmospheric pressure is linked to slightly lower surge heights. Wind speed components showed weak negative correlations, with horizontal wind speed (W_x) at -0.14 and vertical wind speed (W_y) at -0.12, suggesting that higher wind speeds in these directions are mildly associated with lower surge levels. Air temperature showed a very weak negative correlation of -0.03, indicating minimal influence on surge variations.

Table 4. Matrix of correlation coefficients between surge and metrological conditions at Port Said

Condition	W_x (m/s)	Wy (m/s)	Air temperature (°C)	Atmospheric pressure (hpa)	Surge
W_x (m/s)	1.00	**0.95**	**0.15**	**0.07**	**-0.14**
W_y (m/s)	**0.95**	1.00	**0.1**	**0.09**	**-0.12**
Air Temperature(°C)	**0.15**	**0.1**	1.00	**-0.67**	**-0.03**
Atmospheric Pressure (hpa)	**0.07**	**0.09**	**-0.67**	1.00	**-0.18**
Surge	**-0.14**	**-0.12**	**-0.03**	**-0.18**	1.00

While these correlations indicate some influence, their weak nature suggests that surge dynamics at Port Said Harbor are not solely driven by local meteorological conditions. Factors such as bathymetry, coastal geometry, wave-current interactions, and local harbour structures, likely contribute to surge behavior. Future research should look into regional climate drivers, such as teleconnections with the North Atlantic oscillation (NAO) or Mediterranean atmospheric oscillations, to better understand their impact. The semi-enclosed nature of the Mediterranean, along with local bathymetric features, may reduce the rapid influence of climatic variations on surge levels. Future studies could benefit from including hydrodynamic modeling to quantify these contributions. These findings emphasize the need for a more comprehensive approach incorporating additional physical parameters to improve predictive accuracy.

4.4. Empirical equation

To understand the impact of weather conditions on surge heights, an equation has been developed to predict surge levels based on atmospheric pressure and wind components. This method is similar to the approach used by **El-Geziry and Dabbous (2021)**, who also applied multi-regression analysis to model surge changes. Our equation is as follows:

$$\text{Surge (m)} = 4.0796 - 0.0033 \times \text{SLP} - 0.0174 \times W_x + 0.0037 \times W_y \qquad (6)$$

Where, SLP is the sea-level pressure (hPa), W_x is the parallel wind component (m/s), W_y is the normal wind component (m/s). In this equation, atmospheric pressure (hPa) and wind speeds in the W_x and W_y directions (m/s) each contribute to changes in surge heights. A decrease in atmospheric pressure and parallel wind speed correlates with higher surge levels, while an increase in the normal wind speed slightly raises surge levels. The regression coefficient R^2=0.0521 suggests that these variables collectively explain approximately 5.21% of the variation in surge heights, indicating that other factors not included in this model also significantly contribute to surge behavior. These factors may comprise the local bathymetry and coastal morphology, which influence wave-surge interactions, the large-scale atmospheric patterns (e.g., ENSO, NAO) that might contribute to surge variability, and lastly the steric effect that rises from changes in hydrographic parameters. Changes in sea surface temperature and salinity can impact water density and circulation, which can in turn, impact the surge regime. The standard error of 9 cm shows that the predicted surge heights deviate, on average, by 9cm from the observed values.

CONCLUSION

In conclusion, this study emphasizes the dominant role of surge dynamics and meteorological factors (98.66%) in shaping sea-level variations at Port Said Harbor, Egypt, with tidal effects contributing only 1.34%. Atmospheric pressure and wind are the main drivers of surge events, which significantly influence sea-level behavior. The MSL was recorded at 70.36cm, while the MTL was slightly lower at 70.33cm, showing a 3cm difference. The semidiurnal tidal regime, characterized by an F-factor of 0.215 and distinct seasonal variations, provides a foundation for future hydrographic and maritime research, as well as chart production. By offering accurate tidal datum calculations and connecting meteorological conditions to surge dynamics, this research enhances the understanding of regional sea-level changes. These findings are essential for coastal infrastructure planning, flood warning systems, and safe navigation in shallow waters. They also enhance maritime operations in the Mediterranean and the northern entrance of the Suez Canal. Rising water levels can aid larger vessels but may disrupt docking and cargo handling during sudden surges. Effective management is key to maintaining safety and efficiency. To adapt, the port should improve tide and surge monitoring, strengthen infrastructure, and use accurate sea-level forecasts to minimize risks and optimize operations.

While the current work establishes a solid foundation for understanding sea level changes, tidal behavior, and storm surges, improvements to forecasting models and their applications in coastal planning can improve predicted accuracy and usefulness. Recommendations from the present work can be pointed out as:

- **Regular update of tidal datums**: Tidal datums at Port Said Harbor should be revised every 25 years using a certified national grid, following NOAA NOS and CO-OPS policies **(Hicks, 2006)**.
- **Expansion of tide gauge networks**: More tide stations should be established and integrated into a national network to enable real-time sea-level monitoring. This ensures accurate S-100 electronic charts, particularly S-104, for dynamic water level updates and safer navigation.
- **Implementation of real-time data transmission**: Tide stations should include real-time data transmission for continuous monitoring, following GLOSS recommendations **(IOC-UNESCO, 2012)**.
- **Install redundant systems**: Backup water level sensors (e.g., pressure-based or float gauges) should be added for cross-verification.

- **Standardization of tidal datums and gauge settings**: A unified tidal datum and standardized settings across all tide gauges will ensure reliable data exchange, improving S-100 framework applications like S-104 for real-time depth updates.
- **Integration of advanced surge forecasting models:** Machine learning, satellite data, and hydrodynamic modeling should be incorporated to enhance surge prediction accuracy and account for factors like bathymetry, wave interactions, and storm dynamics.
- **Enhancing maritime applications**: Findings should be applied to coastal infrastructure planning, port operations, and disaster risk reduction to improve resilience and safety.

These developments will enhance coastal planning, maritime safety, disaster preparedness, and climate resilience, ensuring long-term growth throughout Egypt's Mediterranean coastline.

REFERENCES

Alam El-Din, K.A.; Abdelrahman, S.M. and El Meligy, M. (2007). Seasonal and long-term variations of sea level and meteorological conditions along the Egyptian coasts. Proc. 8th Int. Conf. Med. Coast. Environ., MEDCOAST (7): 1295-1307.

Burgette, R.J.; Watson, C.S.; Church, J.A.; White, N.J.; Tregoning, P. and Coleman, R. (2013). Characterizing and minimizing the effects of noise in tide gauge time series: relative and geocentric sea level rise around Australia. Geophys. J. Int., 194 (2): 719-736.

Cabanes, C.; Cazenave, A. and Le Provost, C. (2001). Sea level rise during past 40 years determined from satellite and in situ observations. Sci., 294 (5543): 840-842.

Doodson, A.T. (1957). The analysis and prediction of tides in shallow water. Int. Hydrogr. Rev., 41: 85-128.

Egyptian General Authority for Shore Protection. (2015). Coastal Protection Projects along the Mediterranean Coastline. Ministry of Water Resources and Irrigation, Egypt.

Eid, F.M.; Sharaf El-Din, S.H. and Alam El-Din, K.A. (1997). Sea-level variation along the Suez Canal. Estuar. Coast. Shelf Sci., 44 (5): 613-619.

El-Ashmawy, N.; El-Gamal, F. and Lakkis, S. (2017). Impacts of coastal changes on the vulnerability of Port Said, Egypt. In: Finkl, C.W., Makowski, C. (Eds.), Coastal Hazards: Perception, Susceptibility and Mitigation. Springer Int. Publish.: 185-206.

El Fishawi, N.M. (1993). Recent sea level changes and their implications along the Nile Delta Coast. Int. Workshop on Sea-level Changes and their Consequences for Hydrology and Water Management, Noordwijberhout, Netherlands.

El-Geziry, T.M. (2020). On the vulnerability of the Egyptian Mediterranean Coast tothe sea level rise. Athens J. Sci., 7 (4): 195–206.

El-Geziry, T.M. and El-Wakeel, Y.M. (2023). A decadal sea-level variability in Port-Said Harbour (Egypt). Egypt. J. Aquat. Res., 49 (1): 33-39.

El-Geziry, T. and Radwan, A. (2012). Sea level analysis off Alexandria, Egypt. Egypt. J. Aquat. Res., 38: 1–5.

El-Geziry, T.M. and Said, M.A. (2020). Spatial variations of sea level along the Egyptian Mediterranean Coast. Athens J. Med. Stud., 6 (2):141–154.

El-Geziry, T.M.; Dabbous, A.S.; Abdallah, A.M. and Eid, F.M. (2021). Temporal variability of sea-level in Safaga Harbour, Egypt in relation with meteorological conditions and tidal characteristics. Arab. J. Geosci., 14 (13): 1206.

El-Raey, M.; Frihy, O.; Nasr, S.M. and Dewidar, K.H. (1999). Vulnerability assessment of sea level rise over Port Said Governorate, Egypt. Environ. Monitor. Assess., 56: 113-128.

Frihy, O.; Deabes, E.A.; Shereet, S.M. and Abdalla, F.A. (2010). Alexandria-Nile Delta coast, Egypt: update and future projection of relative sea-level rise. Environ. Earth Sci., 61: 253-273.

Gomis, D.; Ruiz, S.; Sotillo, M.G.; Álvarez-Fanjul, E. and Terradas, J. (2008). Low frequency Mediterranean Sea level variability: The contribution of atmospheric pressure and wind. Glob. Planet. Chang., 63: 215–229.

Helmy, M. and Khedr, A. (2024). Sea Level Tidal Attributes in Port Said Harbor, Eastern Egyptian Mediterranean Coast. Trans. Marit. Sci. 13 (2): 1-14.

Hicks, S.D. (2006). Understanding tides. NOAA National Ocean Service, 66p.

Hussein, M.; Moursy, Z. and Tayel, M. (2010). General pattern of Alexandria western harbor sea level change. JKAU: Mar. Sci., 21 (2): 47–61.

Ibrahim, O. and El-Gindy, A. (2022). Comprehensive analysis of monthly mean sea level in the Eastern Mediterranean as a tool for prediction and risk assessment of future expected sea level rise. Arab. J. Geosci., 15: 3.

IOC-UNESCO, (2012). The Global Sea-Level Observing System (GLOSS) Implementation Plan 2012. IOC Tec. Ser., 100: 41p.

Khedr, A.M.; Salama, N.M.; Helmy, M.M. and ELHalawany, H.A. (2022). Tidal Datum Levels Realization based on observed Sea level data analysis in Port Said, Egypt. AIN Journal, 44: 31-38.

Manual on Sea-level Measurement and Interpretation (2006). IOC-Volume IV update to 2006, 78 pp.

Mobarek, I.E. and Anis, A.A. (1974). Standardization of the datum plane in Egypt. Bull. Fac. Eng. Cairo Uni. (17): 1-12.

Mohamed, B.; Mohamed, A.; Alam El-Din, K.A.; Nagy, H. and Elsherbiny, A. (2019). Sea level changes and vertical land motion from altimetry and tide gauges in the Southern Levantine Basin. J. Geodyn., 128: 1-10.

Moursy, Z.A. (1998). Characteristics of the tides at the two main harbors of Egypt. JKAU: Mar. Sci., 9 (1): 19-27.

Oddo, P.; Bonaduce, A.; Pinardi, N. and Guarnieri, A. (2014). Sensitivity of the Mediterranean sea level to atmospheric pressure and free surface elevation numerical formulation in NEMO. Geosci. Mod. Develop. 7: 3001–3015.

Pawlowicz, R.; Beardsley, B. and Lentz, S. (2002). Classical tidal harmonic analysis including error estimates in MATLAB using T_TIDE. Comp. Geosci., 28: 929–937.

Pugh, D.T. (1987). Tides, surges and mean sea level. John Wiley and Sons Ltd., 472p.

Pugh, D.T. (2004). Changing sea levels: Effects of tides, weather and climate. Cambridge University Press, 280p.

Pugh, D. and Woodworth, P. (2014). Sea-level science: understanding tides, surges, tsunamis and mean sea-level changes. Cambridge University Press, 395p.

Radwan, A.M.; Magdy, M.; Rabah, M.; Saber, A.Y. and Zaki, A. (2021). Sea level analysis using tide gauge observations at the northern delta coast, Egypt. NRIAG J. Astron. Geophys., 10 (1): 361–371.

Saad, N.N.; Moursy, Z.A. and Sharaf El-Din, S.H. (2011). Water heights and weather regimes at Alexandria Harbor. Int.J. Phys. Sci., 6 (30): 7035–7043.

Sharaf El Din, S.H.; Ahmed, K.A;, Khafagy, A.A.; Fanos, A.M. and Ibrahim, A.M. (1989). Extreme sea level values on the Egyptian Mediterranean coast for 50 years. International Seminar on Climatic Fluctuations and Water Management, 15p.

Shaker, A.; Alnaggar, D.; Saad, A. and Faisal, H. (2009). The Relationship between Mean Sea Levels of the Mediterranean and the Red Sea through Port Said and Sues. Proc. Int. Conf. Arab Union Survey., Lebanon: 1-13.

Shalaby, M. (2000). Wave and surge forecasting along the Egyptian Coast of the Mediterranean Sea. MSc. Thesis. Arab Academy for Science, Technology and Maritime Transport, Alexandria, Egypt.

Svensson, C. and Jones, D.A. (2004). Dependence between sea surge, river flow and precipitation in south and west Britain. Hydrol. Earth Sys. Sci., 8 (5): 973-992.

Tonbol, K. and Shaltout, M. (2013). Tidal and non-tidal sea level off Port Said, Nile Delta, Egypt. JKAU: Mar. Sci., 24 (2): 69-83.

Tsimplis, M.N.; Alvarez-Fanjul, E.; Gomis, D.; Fenoglio-Marc, L., and Perez, B. (2005). Mediterranean Sea level trends: Atmospheric pressure and wind contribution. Geophys. Res. Let., 32: L20602.

UNEP. (2021). The Global Status Report on Sea-Level Rise. United Nations Environment Programme.

United Nations Conference on Trade and Development (UNCTAD). (2021). Case study 3: Port of Port Said, Egypt.

Weis, J.S.; Watson, E.B.; Ravit, B.; Harman, C. and Yepsen, M. (2021). The status and future of tidal marshes in New Jersey faced with sea level rise. Anthrop. Coasts, 4 (1): 168-192.

World Meteorological Organization (WMO). (2024). Annual Climate Review for the Mediterranean Region.